

U.S. copyright law (title 17 of U.S. code) governs the reproduction and redistribution of copyrighted material.

PENDING - Lender



33223575

GENERAL RECORD INFORMATION

Request Identifier: **33223575** Status: PENDING 20070824
 Request Date: 20070824 Source: FSILLSTF
 OCLC Number: 53832943 AUG 24 2007
 Borrower: **GIE** Need Before: 20070831 SENT BY ARIEL
 Receive Date: Renewal Request:
 Due Date: New Due Date:
 Lenders: *MWR, FER, FNN
 Request Type: Copy

BIBLIOGRAPHIC INFORMATION

Call Number:

Author: Barnes, William L.
 Title: Earth observing systems VIII : 3-6 August, 2003, San Diego, California, USA
 ISBN: 9780819450241
 Imprint: Bellingham, Wash. : SPIE, 2003
 Article: Vicarious calibration of Aqua and Terra MODIS/Thome, K.J.
 Volume: 5151
 Date: 2003
 Pages: 395-405
 Verified: WorldCat Desc: x, 634 p. : Type: Book

BORROWING INFORMATION

Patron: G. Chander
 Ship To: U.S. Geological Survey-EROS/ATTN: Library/Mundt Federal Bldg./Sioux Falls, SD
 57198-0001
 Bill To: same
 Ship Via: E-mail/fax preferred.
 Electronic Delivery:
 Maximum Cost: IFM - 20.00
 Copyright Compliance: CCL
 Billing Notes: IFM please; invoices not accepted. We do not charge. Thanks!
 Fax: 605-594-2725
 Email: cdeering@usgs.gov
 Affiliation: FEDL, LVIS
 Borrowing Notes: Please send via e-mail to cdeering@usgs.gov.

LENDING INFORMATION

email GIE

VICARIOUS CALIBRATION OF AQUA AND TERRA MODIS

K. Thome, J. Czapla-Myers, S. Biggar

Remote Sensing Group, Optical Sciences Center, University of Arizona, Tucson AZ 85721

ABSTRACT

The Moderate Resolution Imaging Spectroradiometer (MODIS) is onboard both the Terra and Aqua platforms. An important aspect of the use of MODIS, and other Earth Science Enterprise sensors, has been the characterization and calibration of the sensors and validation of their data products. The Remote Sensing Group at the University of Arizona has been active in this area through the use of ground-based test sites. This paper presents the results from the reflectance-base approach using the Railroad Valley Playa test site in Nevada for both Aqua and Terra MODIS. The key to the approach is the measurement of surface reflectance over a 1-km² area of the playa and results from this method shows agreement with both MODIS sensors to better than 5%. Early results indicate that while the two sensors both agree with the ground-based measurements to within the uncertainties of the reflectance-based approach, there were significant differences between the Aqua and Terra MODIS for data prior to September 2002. Recent results indicate that this bias, if any, is now within the uncertainties of the reflectance-based method of calibration.

Keywords: Absolute-radiometric calibration, vicarious calibration, atmospheric correction

1. INTRODUCTION

The launch of Landsat-7 in April 1999 started a sequence of launches of an unprecedented number of earth-imaging sensors put into orbit for both land-based and ocean-based remote sensing. These include sensors ranging in spatial resolution from 0.6 to 1000 m and spectral resolution ranging from multispectral to hyperspectral spanning the wavelength regions from visible, near-infrared, through the thermal infrared and beyond to radar wavelengths. Swath widths and repeat visits also span a wide range of values all leading to an opportunity to study earth-processes on a global scale. A good example of one of these sensors was the launch of the Moderate Resolution Imaging Spectroradiometer (MODIS) on the Terra platform in December 1999 and on the Aqua platform launched in May 2002. The MODIS is one of five sensors onboard the Terra platform and one of four sensors on the Aqua platform. Both platforms are part of NASA's Earth Observing System (EOS) with the sensors on the Terra platform providing data from a morning crossing time in a descending mode and Aqua having an afternoon crossing time in ascending mode.¹ The two MODIS sensors are identical in design with 36 spectral bands covering the visible and near infrared portion to the thermal infrared. The spatial resolution of the sensor varies with spectral band with values of 250 m, 500 m, and 1000 m depending upon the specific application and signal-to-noise characteristics of the particular band.

One of the primary efforts to the use of MODIS data is to develop synergy between the morning and afternoon data sets to improve understanding of land, ocean, and atmospheric processes. This type of work clearly requires that data from the two sensors are consistent from a radiometric standpoint. That is, the two sensors should report the same band-averaged spectral radiances when subject to the same input spectral radiances. Such consistency necessitates an accurate radiometric calibration of the two MODIS. While both sensors were built, characterized, and calibrated by SBRS (Santa Barbara Remote Sensing) prior to launch, it is expected that both sensors could degrade once on orbit. Thus, the use of onboard calibration techniques is integral to the accurate retrieval of at-sensor spectral radiance throughout the lifetime of both sensors.

Unfortunately, it is still possible that biases could exist between the sensors due to the nearly three years between their characterizations and launches. Thus, it is required to rely on vicarious approaches to ensure that data from the two separate sensors are consistent because it is not possible to do inflight cross-calibration between the two MODIS using onboard approaches. The Remote Sensing Group (RSG) at the University of Arizona has exploited these vicarious

THIS MATERIAL MAY BE PROTECTED BY US
COPYRIGHT LAW (TITLE US CODE 17). THE
REQUESTER IS LIABLE FOR INFRINGEMENT.

methods to calibrate both low- and high-spatial-resolution sensors with accuracies in the 2-5% range.^{2,3,4,5,6,7,8} Application of these approaches to MODIS required modification to account for the much larger spatial resolution of the 1-km bands of the sensor. This work briefly describes these modifications and presents results of applying the reflectance-based approach to MODIS on both the Aqua and Terra platforms. Early data sets from the Aqua platform sensor indicated a possible bias between the two MODIS sensors, but more recent results shows that any bias is well within the uncertainties of the vicarious calibration approach. Comparison of the early Aqua MODIS results to data collected for other sensors indicates that the ground data were not in error, thus it is not clear at this stage for the reason for the disparity between the vicarious predictions of at-sensor radiance and those reported by Aqua MODIS. The results from both Terra and Aqua MODIS agree with the vicarious results to an accuracy of better than +/-3% in most bands and both sensors show good agreement with Landsat-7 ETM+ when using the vicarious calibration as a proxy for cross-calibration.

2. RAILROAD VALLEY TEST SITE

The test site used in this work is the Railroad Valley Playa that is on Bureau of Land Management land in central Nevada. The overall size of the playa is approximately 15 km by 15 km at an elevation of approximately 1.5 km. The RSG has been using this site for the radiometric calibration of terrestrial imagers since 1998. The playa's location in a region with high expectations of clear weather and low aerosol loading, coupled with the surface's high reflectance, makes it a good site for the reflectance-based approach described below. Ground-based atmospheric measurements are made at a latitude and longitude of 38.504 degrees North and 115.692 degrees West. The test site that the RSG uses for the reflectance-based calibration of sensors with spatial resolutions of 50 m or less is located approximately 100 m to the east of the atmospheric measurements. The center of the area used for the reflectance-based calibration of large footprint sensors is located at 38.497 North and 115.691 West, approximately 700 m south of the atmospheric instrumentation. This area has been measured consistently since 2000.

Figure 1 shows a full-scene, 185-km wide swath, ETM+ image with Railroad Valley Playa highlighted by the outer box in the lower portion of the figure. The inner box in this figure highlights the region of the playa that is shown in the image in Figure 2. This image is from Space Imaging's Ikonos sensor supplied via NASA's Commercial Data Buy with a spatial resolution of approximately 1 m. The areas of the playa used by the RSG for its work are indicated in this figure. Figure 3 shows a Terra MODIS 500-m resolution image of the playa. While it is clear that surface features plainly evident in the high-resolution data sets are no longer evident in the MODIS imagery, boundaries of the playa, and spatial features in the playa make locating specific regions of the playa possible in the MODIS data. Using ground control points in the MODIS and ETM+ images along with the geolocation information supplied with the MODIS data, makes it possible to locate the low-resolution test site to better than a pixel in the MODIS imagery.

Typical atmospheric conditions at the site include an aerosol optical depth at 550 nm that is less than 0.05 and horizontal visibilities in excess of 60 km. Measurements of atmospheric aerosols using solar radiometer techniques show that variations over time of the optical depth are typically at the noise level of the measurements. Since these measurements typically cover >4 hours, it implies that the horizontal variability of the aerosols over the playa is quite small for a normal, clear-sky day. However, aerosols can vary dramatically across the playa on dates for which clouds are present and for dates on which there are extreme wind conditions. Peak precipitation occurs in winter between December and March and also during the summer months of July and August. There is an additional feature to the Railroad Valley site that is not seen at other test sites used by the RSG. This is that a large amount of aircraft contrails can form and then dominate the sky under conditions that might normally have clear skies or very thin cirrus. The contrails are a result of the large amount of commercial aircraft traveling to and from the west coast that are forced over the playa area by several military air space restrictions that are south of Railroad Valley.

The reflectance of the playa is generally greater than 0.3 and relatively flat spectrally except for the blue portion of the spectrum and an absorption feature in the shortwave infrared (an example of the spectral reflectance can be seen in Figure 8). Ideally, this reflectance would be constant throughout the year, but experience with this site shows that there are significant changes in reflectance with changes in surface moisture. These effects occur primarily in the winter months from large-scale weather systems and in summer months from periodic episodes of heavy rain. Ground-based

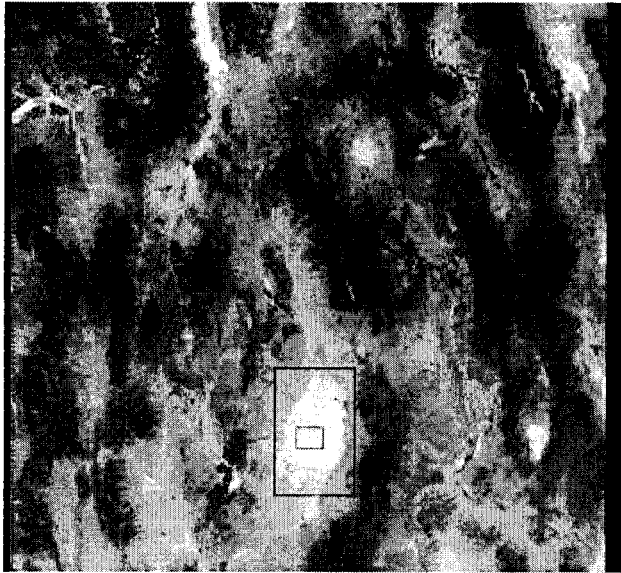


Figure 1. Landsat-7 ETM+ band 2 full-scene image (185-km swath) showing the Railroad Valley Playa at the lower-center portion of the image. Inside box indicates general area of playa used here.

measurements of the directional reflectance characteristics of the playa show it to be nearly lambertian out to view angles of 30 degrees for incident solar zenith angles seen for overpasses of Terra and Aqua. All of these factors are critical to reducing the uncertainties of a cross-calibration method.⁹

3. REFLECTANCE-BASED APPROACH

3.1 Method summary

The reflectance-based method has been described previously^{2,3,7} and is not given in detail here. The method relies on characterizing the surface of a test site and the atmosphere over that test site and using the results of these characterizations in a radiative transfer code to predict at-sensor radiance. The approach has been in use since 1984 when it was first applied to Landsat-5 Thematic Mapper.^{2,3} These early applications focused on applying the method to high-spatial resolution sensors (<50-m spatial resolution). Application to sensors such as MODIS where the ground-pixel size is significantly larger creates problems for both the measurement of the surface reflectance that is used in the radiative transfer code as well as the measurements of atmospheric conditions.

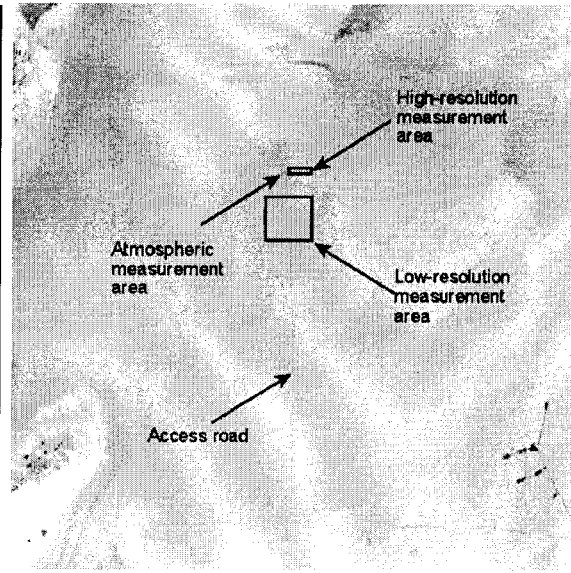


Figure 2. Space Imaging's Ikonos band 2 image of Railroad Valley Playa. Relevant points are noted in the image. Dark structures in lower right are oil well pads and access roads.



Figure 3. Terra MODIS band 4 image of Railroad Valley Playa at 500-m spatial resolution. Outline of the playa is clearly visible as well as other features in the image.

3.2 Reflectance retrieval and spatial sampling

The original approach for retrieving surface reflectance in the case of small-footprint sensors, such as Landsat-7 Enhanced Thematic Mapper Plus (ETM+), relied on transporting a spectroradiometer across a rectangular area as shown in Figure 4.¹⁰ In this figure, the path walked by the operator of the spectroradiometer is indicated by the dashed lines within the Landsat test site. Also shown to scale is the size of a 1-km footprint similar to the nadir-viewing resolution of the low-spatial-resolution bands of MODIS. The 16 dotted lines in the figure correspond to 16 rows of ETM+ data and the width of the site corresponds to four columns of data. Thus, a total of 64 ETM+ pixels are characterized in this case.

This approach for ETM+ of measuring 120 m × 480 m broken into 64 areas that are 30 m × 30 m is to ensure sampling an area corresponding to a large number of the detectors for the sensor (all 16 in this case). It also allows the homogeneity of the surface to be assessed so that errors in site registration to the image data can be determined. The data collection process from the area shown in Figure 4 takes approximately 40 minutes with a total distance walked of 1.9 km. The length of time needed to cover this amount of ground is determined primarily by the data collection rate of the spectroradiometer set by the user.

In the case of MODIS, one could collect data over the identical site as that used for smaller-footprint sensors and then assume that these measurements of the small area are applicable to a much larger area related to a 1-km pixel. Unfortunately, the regions where our current test sites are located do not lend themselves to this approach due to surface inhomogeneity. Another approach is to sample a larger area of the test site with the same sampling strategy as for the small footprint sensors. Obviously, dividing a 1-km by 1-km area into 30-m subareas is not feasible since it would require measuring nearly 1100 subareas. This would take approximately 11 hours.

A more reasonable approach would be to subdivide the large area into the same 64 pixel subareas collecting 10 samples within each area. The smallest size of the overall site would be 1 km × 1 km. In this case, each subarea is about 130 m × 130 m. This approach still has two problems. First is that it is logistically difficult to transport the reference standard that is used to convert these data into reflectance over the distances that are necessary in this case. When working with the smaller site the reference standard is measured at every other dotted line, requiring the reference to be moved seven times over a total distance of 420 m. Moving the reference more than twice this distance would be non-trivial, especially at air temperatures over 310 K. Second, and more importantly, is that the total distance walked is more than 8 km. This would take someone walking at a rapid pace nearly two hours to complete, which is longer than desired and makes the data susceptible to changes in illumination conditions due to changing sun angle and atmospheric conditions such as clouds.

The goal is to keep the measurement time to about one hour, thus the limit to the linear distance covered is about 4 km. This limits the work to four transects in order to sample a 1-km × 1-km area. One option is to have all four lines parallel to one another. This has the logistical problem of moving the reference standard. The approach that has been adopted is that shown in Figure 5 and consists of four pairs of transects oriented 90° to each other in approximately the along- and cross-track directions. This approach has the advantage of attempting to characterize broad scale changes in the site in orthogonal directions. The disadvantage to this method is that the sampling could be inadequate to properly characterize the reflectance of a full MODIS pixel.

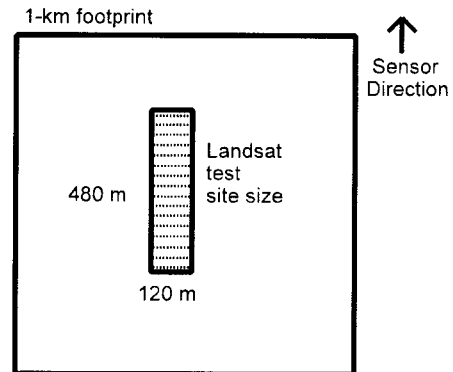


Figure 4. Schematic showing size of a typical test site used for vicarious calibration of a small-footprint sensor (ETM+). 1-km footprint is shown for reference. Dotted lines within Landsat site indicate paths walked to sample surface reflectance.

3.3 Atmospheric characterization issues

The other primary inputs to the radiative transfer code are the atmospheric conditions at the time of sensor overpass. In the past, it has been assumed that the atmospheric data are constant over the entire test site based on a set of point measurements near the site. Applying this assumption to the larger footprint case should not significantly increase the error since typical calibration days have non-varying atmospheric conditions. However, this effect can be significant in the case of cloudy conditions, especially those for which there would be sub-pixel clouds. Additional uncertainties arise from MODIS's large field of view allowing it to image a site at large view angles. These large view angles require a much better characterization of atmospheric effects due to the longer view path and an improvement in the characterization of the surface bi-directional reflectance.

Application of the reflectance-based approach to the Terra MODIS sensor has shown that the uncertainties are similar in the large footprint case as they are for small footprints. The precision of the results for the large footprint case is not as good as for small footprint sensors, and this is most likely due to uncertainties in the registration of the ground data to the imagery.^{7,8,11}

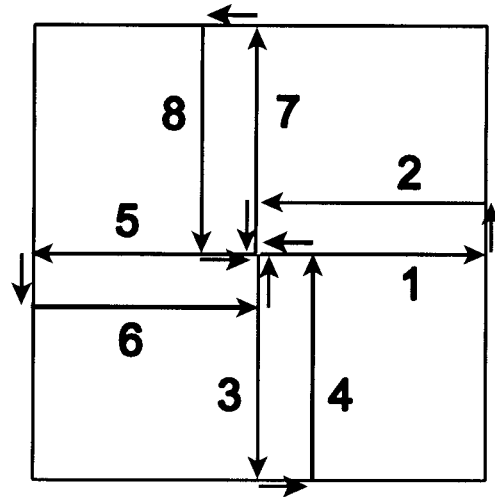


Figure 5. Path walked for collection of surface reflectance data of a 1-km by 1-km area. Numbers indicate the order in which the longer paths are walked. Each longer path is 500 m and shorter arrows indicate 100-m distances.

4. RESULTS

The primary results presented here are for 10 dates collected for Aqua MODIS between July 2002 and April 2003. The dates of successful calibrations are listed in Table 1, which also includes the sun angle and sensor view angle information.

Date	Solar angles		View angles		Junge Parameter	550 nm aerosol optical depth	Column water vapor (cm)	Column ozone (cm-atm)
	Zenith	Azimuth	Zenith	Azimuth				
2002-07-13	21.7	224	3.3	257	3.71	0.147	1.77	0.396
2002-08-12	29.2	221	25.9	259	3.92	0.237	1.31	0.596
2002-08-14	28.2	215	3.6	260	3.98	0.054	1.27	0.464
2002-08-16	27.6	209	19.7	75	4.03	0.289	1.37	0.635
2002-09-22	42.7	211	13.6	260	3.68	0.026	1.19	0.362
2002-11-02	57.0	205	4.3	256	3.16	0.021	0.35	0.121
2002-12-04	63.5	200	4.4	257	2.56	0.023	0.77	0.225
2003-01-19	61.0	199	26.6	259	3.08	0.024	1.00	0.147
2003-02-22	50.3	198	4.4	256	2.55	0.045	0.71	0.276
2003-04-11	33.7	211	4.4	257	2.82	0.126	0.98	0.205

In addition to the dates presented here, an additional 4 dates of collections were also attempted during this period but were not successful due to poor weather conditions. The dates of the unsuccessful collections were July 11 and 15, August 19, and March 19. As can be seen from the table, all of the successful collections had view angles by the Aqua MODIS sensor of less than 30 degrees and six of the dates were at the nadir look for the Railroad Valley test site and the orbit of Aqua.

Also included in Table 1 are the atmospheric conditions from all of the dates. The Junge parameter given in the table is related to the size distribution of aerosols in the atmosphere. A larger value indicates that the atmosphere is dominated by smaller particles. A typical value for the Junge parameter is 3.0 and it is derived here from the slope of the best fit line to the aerosol optical depths retrieved from solar transmittance measurements.¹² An example of this is shown in Figures 6 and 7. Each point on the graphs represents a different spectral band in the solar radiometer used to determine the spectral transmittance of the atmosphere. All of the data shown have been corrected for molecular scattering. The large spike near 1 μm in both figures (relating to band 9 of the instrument) is due to water vapor absorption. The larger optical depths in bands 4-6 are due to ozone absorption. The error bars shown in the graphs correspond to a 5% uncertainty that is nearly twice what is expected from the uncertainty in the instrument calibration. The dashed lines in the figures relate to the 1- σ standard deviation about the 10-minute average of the data. The solar transmittance data in both cases were collected at 1-minute intervals, thus each graph represents the average and standard deviation of 11 data points.

Note that in the case of the data on August 14, 2002 the atmospheric variability is less than the instrumental uncertainty while for February 22, 2003 the atmospheric variability is similar to, or greater than, the instrumental uncertainty. Another point to note in the graphs is that the total aerosol optical depth near 550 nm is similar for both dates while the slopes of the two line fits are significantly different. This results from two different atmospheric regimes on the two separate dates. In the case of August 14, the atmosphere was dominated by smoke particles from large wildfires in California. The February date, on the other hand, was marked by excellent horizontal visibilities but high, thin cirrus clouds were present as seen by the large standard deviations indicating the spatial heterogeneity of the clouds. In addition, the smaller slope of the line fit indicating the presence of larger particles.

This explanation of the Junge parameter is then useful to understand the last three columns in Table 1. The data in all three of these columns are derived with reference to the straight-line fit of the Junge parameter. The 550-nm aerosol optical depth is the value of the optical depth derived from the line fit at 550 nm. The column water vapor and ozone are derived by determining the difference between the straight-line fit and the measured optical depth and then converting

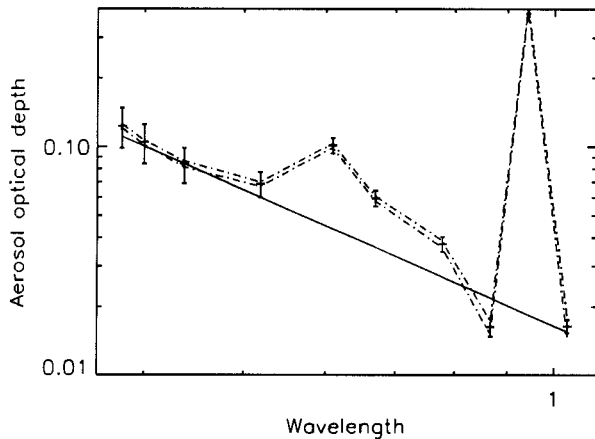


Figure 6. Absorption and aerosol optical depths as a function of wavelength for 2002-08-14 for a 10-minute average about the Aqua platform overpass at Railroad Valley. Also shown is best fit line to the inferred aerosol optical depth.

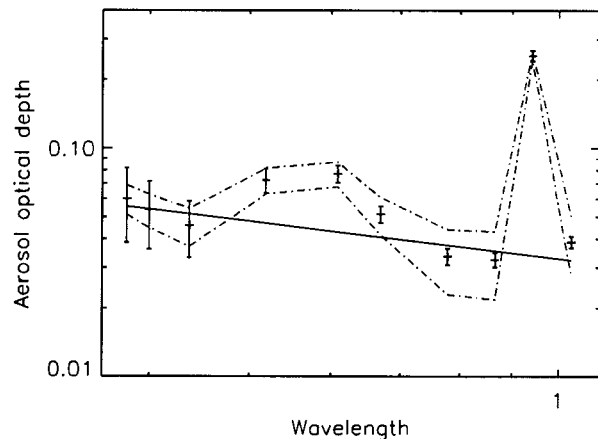


Figure 7. Absorption and aerosol optical depths as a function of wavelength for 2003-02-22 for a 10-minute average about the Aqua platform overpass at Railroad Valley. Also shown is best fit line to the inferred aerosol optical depth.

these differences to absorber amount via an appropriate model.^{12,13} Viewing the results in the table shows that the aerosol loading between dates varied significantly with the lowest values approaching 0.02 and the highest values in July and August 2002 related to the previously-mentioned smoke particles. The higher optical depth on April 11, 2003 was due to the presence of clouds. Column ozone also varied widely during the period, but it is expected that much of this variation is due to uncertainties in the retrieval method rather than real changes in the column ozone amount.

The reflectance results are summarized in Table 2 showing the band-averaged reflectance of each of the MODIS bands calibrated here. Of note is the variation in reflectance as a function of time primarily due to changing surface moisture conditions. Wavelengths shorter than 500 nm typically have a reflectance less than 0.3 with larger reflectance values at longer wavelengths. This is evident in Figure 8 which shows the spectral reflectance derived for the test site used here from measurements on February 22, 2003. High values for reflectance on May 27, 2003 were caused by a thin layer of white salts that are eventually removed through windblown mechanisms. The repeatability of the reflectance measurements is displayed in the table in the three August data sets which all agree to better than 0.5%.

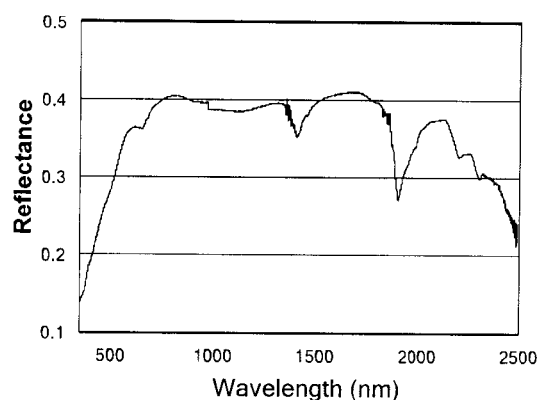


Figure 8. Example spectral reflectance of Railroad Valley Playa test site derived from data collected on February 22, 2003.

The data described above are then used in a radiative transfer code to predict the at-sensor radiance at 1-nm intervals from 350-2500 nm. These hyperspectral, predicted radiances are band-averaged using the appropriate spectral response of a given band to determine the in-band spectral radiance. These predicted radiances are compared to the reported radiance from the MODIS sensor to determine whether the calibration of MODIS is correct. All of the results shown

Table II. Summary of reflectance results for each of the Aqua dates and MODIS bands.										
Date	Band 1	Band 2	Band 3	Band 4	Band 5	Band 6	Band 7	Band 8	Band 9	Band 17
	645 nm	858 nm	469 nm	555 nm	1240 nm	1640 nm	2130 nm	412 nm	443 nm	905 nm
2002-07-13	0.377	0.414	0.264	0.344	0.406	0.436	0.406	0.207	0.240	0.408
2002-08-12	0.455	0.492	0.339	0.424	0.483	0.506	0.467	0.273	0.312	0.488
2002-08-14	0.449	0.488	0.334	0.418	0.483	0.506	0.472	0.270	0.308	0.483
2002-08-16	0.455	0.492	0.339	0.423	0.485	0.507	0.474	0.274	0.313	0.488
2002-09-22	0.400	0.434	0.284	0.364	0.434	0.456	0.430	0.225	0.260	0.430
2002-11-02	0.387	0.423	0.268	0.350	0.424	0.447	0.421	0.210	0.244	0.418
2002-12-04	0.373	0.407	0.261	0.339	0.404	0.418	0.379	0.206	0.238	0.402
2003-01-19	0.366	0.402	0.256	0.331	0.394	0.412	0.387	0.205	0.235	0.398
2003-02-22	0.363	0.402	0.255	0.336	0.391	0.409	0.374	0.198	0.231	0.397
2003-04-11	0.420	0.464	0.299	0.389	0.458	0.477	0.443	0.232	0.272	0.459

here rely on Level-1B data obtained from NASA's EOS Data Gateway. These data correspond to radiometrically-, but not geometrically-corrected data. Data were omitted in all instances when a faulty detector was present over the region of interest. Conversion of the Level-1B digital counts was accomplished using the conversion factor supplied in each individual data set's EOS Hierarchical Data Format (HDF) file.

Figure 9 summarizes the results for Aqua MODIS for all bands listed in Table 2 except for Band 9, which suffers from saturation on all but one of the dates. The results shown in the figure are the percent differences between the vicarious predictions and the reported radiance as a function of date for all of the bands of interest. Figure 10 shows the same results except gives the percent differences as a function of band rather than date.

The results from early in the mission indicate significant differences between the reported and predicted radiances. This difference then decreases dramatically for all data sets after September 22. It is not clear at this point what would cause this effect, but data sets from other sensors in July, August, and September indicate that the ground data were not anomalous. Figure 11 shows that data collected for other sensors during this same time period are clearly different from the results obtained for Aqua MODIS. While the argument can be made that there is a change in equipment, surface parameterization, etc. between the morning and afternoon overpass periods, this would not explain the better results that are obtained after September and the comparably good results from August 14 for Aqua. Further work is underway to understand this behavior.

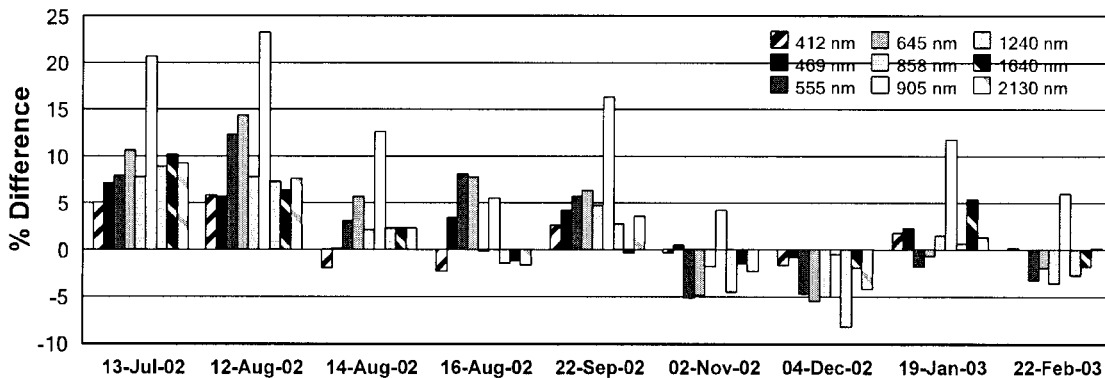


Figure 9. Summary of Aqua MODIS results from Railroad Valley Playa using the reflectance-based approach. Postive percent differences indicate that the reported radiances exceed the predicted values.

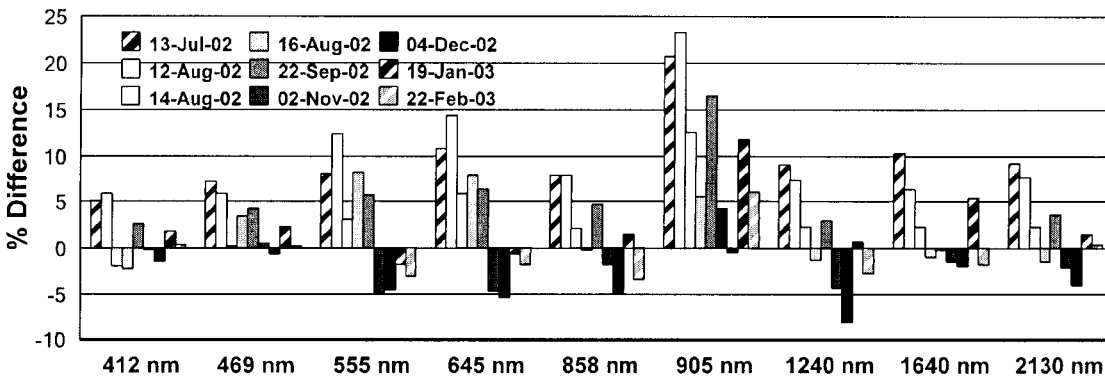


Figure 10. Same as Figure 9 except results are arranged to show percent differences for all dates for a given band

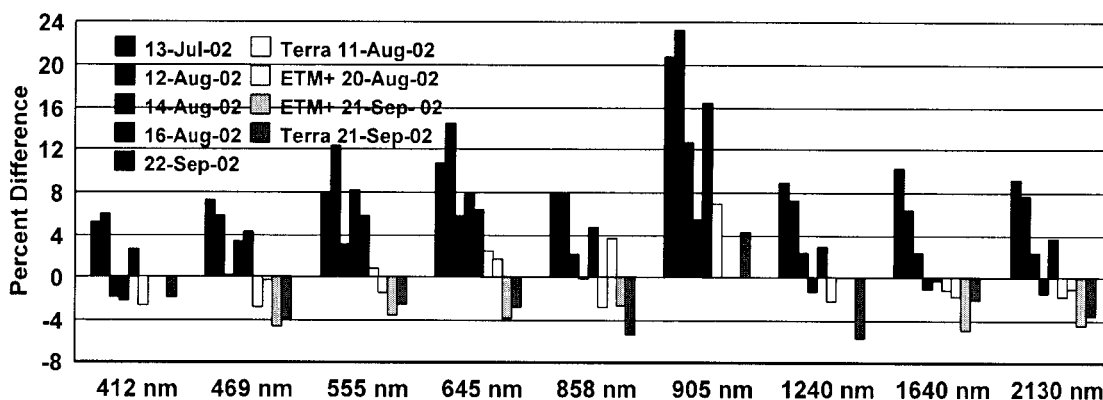


Figure 11. Results from Aqua MODIS from July, August, and September 2002 with ETM+ and Terra MODIS results for the same period.

Further understanding of the Aqua MODIS results can be gained when comparing the average percent difference between the vicarious results and sensors with similar spectral bands. This is shown in Figure 12 in which the average percent difference between Landsat-7 ETM+ and the vicarious results is shown along with the average percent difference for Aqua and Terra MODIS. The Landsat-7 ETM+ results are the average of 39 data sets collected during the period between June 1999 and May 2003. The Terra MODIS results are for the period between April 2000 and September 2002 and consist of 12 data sets. All of the Terra MODIS results are for Railroad Valley, while the ETM+ results contain data sets from all test sites used by the RSG. The Aqua MODIS values are based on the data shown previously. The bars for each sensor indicate the standard deviation about the average for each data set.

The key points to note in Figure 12 are that the standard deviations for the Aqua MODIS sensor are typically larger than those of the Terra MODIS and the averages are higher in general than those of Terra MODIS and ETM+. The larger standard deviation is of interest since the Terra MODIS data set and Aqua MODIS data set consist of nearly the same number of points and similar measurement conditions.

Limiting the Aqua results to include only the five dates after September 22 significantly reduces the standard deviation as well as causes the average percent difference to agree much better with ETM+ and Terra MODIS (see Figure 13). Of interest is also the relatively good agreement between the vicarious and reported radiances with all averages (except 905 nm for Aqua MODIS) in Figure 13 being within 5% of the vicarious predictions. It is not clear at this point the cause

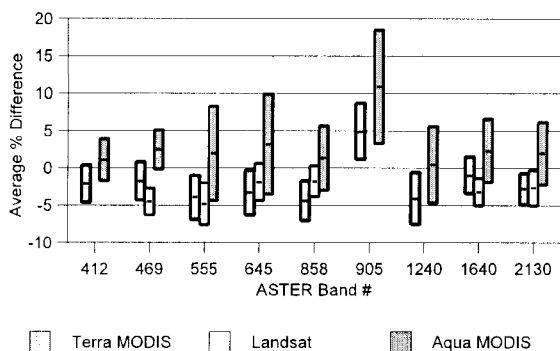


Figure 12. Average percent difference and standard deviation between vicarious predictions and reported sensor radiance for ETM+ and both MODIS sensors.

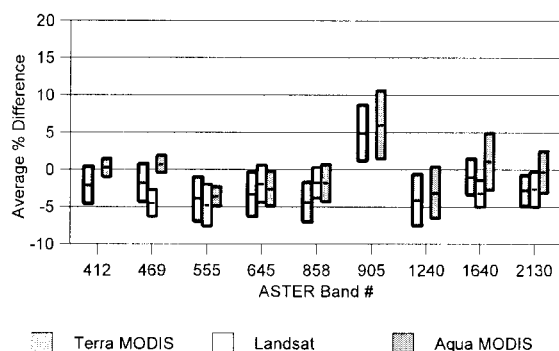


Figure 13. Same as Figure 12 except values for Aqua MODIS are determined from the five data sets collected after September 22.

of the odd behavior of the 905-nm band for both Terra and Aqua MODIS, but one suspected cause is a bias in the surface measurements due to water vapor absorption.

5. UNCERTAINTIES

The primary causes of uncertainties in the reflectance-based approach applied to MODIS are registration of the ground-based measurements of reflectance to the sensor data, spatial heterogeneity in the surface that is not sampled properly by the paths shown in Figure 5, and errors in the retrieved surface reflectance. Errors in the atmospheric characterization and the radiative transfer calculations can also play a role, but are typically not large sources of uncertainty due to the high reflectance of the surface. Surface BRDF effects can also be important, but these are mitigated by limiting the data collections to cases for which MODIS views the surface at angles within 30 degrees of nadir. One key conclusion regarding the uncertainties of the reflectance-based approach is that there should not be a bias between the vicarious results obtained for the morning overpass of Terra MODIS to those of the afternoon overpass of Aqua MODIS.

The spatial uniformity issue is the most important factor since it minimizes the effects of misregistration with the ground data as well as reducing errors due to sampling of the reflectance. Past work to evaluate the suitability of the Railroad Valley site for cross-calibration showed that the effects of misregistration are generally less than 0.5% for the worst case of a 500-m misregistration of the selected area of Railroad Valley. The effect due to misregistration is largest at longer wavelengths beyond 1600 nm. The smallest differences are seen with misregistration in the east-west direction, with a larger difference in the north-south direction with regions to the north of the playa area being darker than areas to the south. For the Aqua data used here, shifting the selected area in the MODIS image by a full pixel had less than a 2% effect on all dates and all bands with most differences less than 0.5%.

Equating the reflectance of a 1-km² area of the playa to that sampled by the paths shown in Figure 5 has been tested using higher-resolution data such as ETM+. While a complete sampling of all dates possible has not been done and the history of ETM+ imagery over the Playa is somewhat limited, sampling issues should not create uncertainties in excess of 0.5%. Of course, this assumes that the entire site is sampled which is not always the case due to user fatigue and instrument malfunctions. For example, the data set used for December 4, 2002 included data along paths 1-4 only. This is not an issue since the choice of ordering of the paths was selected to ensure a representative sampling of the site with paths 5-8 offering to supplement the sites understanding and an adequate understanding of the reflectance can typically be obtained solely from paths 1-4.

Based on the above discussion, it should be clear that for a typical data set, errors due to registration and sampling should be minimal. Other errors in the approach will be similar for the large footprint sensor as they are for the small footprint sensors. Thus, estimates of the uncertainties for the reflectance-based results for the work shown here should be in the 3-5% range with smaller errors in the visible and near infrared. The precision of the results should also be similar as well.

5. CONCLUSIONS

The results shown in Figures 12 and 13 are the most telling. Figure 13 indicates that the two MODIS sensors and ETM+ all agree to within the combined uncertainties of the methods. This neglects the odd results obtained for Aqua MODIS in July, August, and September 2002, which are still under study at the time of this paper. Early indications are that the ground-based measurements are not the cause of the discrepancy since measurements for other sensors for similar times do not show such large differences. It is also not expected that the larger differences are due to an inherent bias caused by the difference in morning and afternoon overpasses, but this is currently under study to verify that this is indeed the case.

A general conclusion that can be reached from this work is that the reflectance-based approach can be applied accurately to large-footprint sensors. Consistent application of this approach to multiple sensors allows for a cross-calibration of these sensors relative to the vicarious results. That is, comparison between Aqua MODIS and the reflectance-based

results allows a bias between the two approaches to be determined. A similar bias between the Terra MODIS and reflectance-based approach can likewise be found. Comparison of the biases for the Terra and Aqua sensors then allows a bias between the two sensors relative to the vicarious results to be found. Such a method will have great utility in the cross-comparison of sensors in the future using sites such as Railroad Valley Playa.

ACKNOWLEDGMENTS

We wish to acknowledge the Bureau of Land Management's Tonopah office for the assistance in gaining access to the Railroad Valley Playa site. We would also like to acknowledge the efforts of the numerous individuals who assisted in collecting the ground-based data used in this work. This research was supported by NASA contract NAS5-31717 and NASA grants NAG5-1139 and NAG5-2448, and the Commercial Data Buy Program at Stennis Space Center.

REFERENCES

1. W. L. Barnes, T. S. Pagano, and V. V. Salomonson, "Prelaunch characteristics of the Moderate Resolution Imaging Spectroradiometer (MODIS) on EOS-AM1," *IEEE Trans. On Geoscience and Remote Sensing*, Vol. 36, pp. 1088-1100, 1998.
2. P. N. Slater, S. F. Biggar, R. G. Holm, R. D. Jackson, Y. Mao, M. S. Moran, J. M. Palmer, and B. Yuan, "Reflectance- and radiance-based methods for the in-flight absolute calibration of multispectral sensors," *Rem. Sens. Env.*, Vol. 22, pp 11-37, 1987.
3. K. J. Thome, D. I. Gellman, R. J. Parada, S. F. Biggar, P. N. Slater, and M. S. Moran, "In-flight radiometric calibration of Landsat-5 Thematic Mapper from 1984 to present," *Proc. of SPIE*, Vol. 1938, 1993.
4. S. F., Biggar, P. N. Slater, and D. I. Gellman, "Uncertainties in the in-flight calibration of sensors with reference to measured ground sites in the 0.4 to 1.1 μm range," *Rem. Sens. Env.*, Vol. 48, pp. 242-252, 1994.
5. P. N. Slater, S. F. Biggar, J. M. Palmer, and K. J. Thome, "Unified approach to pre- and in-flight satellite sensor absolute radiometric calibration," *Proceedings of SPIE*, Vol. 2583, pp. 130-141, 1995.
6. P. M. Teillet, P. N. Slater, T. Ding, R. P. Santer, R. D. Jackson, and M. S. Moran, "Three Methods for the Absolute Calibration of the NOAA AVHRR Sensors In-Flight," *Rem. Sens. Env.*, **31**, pp. 105-120, 1990.
7. K. Thome, N. Smith, K. Scott, "Vicarious calibration of MODIS using Railroad Valley Playa," *International Geoscience and Remote Sensing Symposium*, Sydney, Australia, 2001
8. K. Thome, E. Whittington, and N. Smith, "Radiometric calibration of MODIS with reference to Landsat-7 ETM+," *Proc. SPIE Conf. #4483*, San Diego, Calif., 2001.
9. K. P. Scott, K. J. Thome, and M. R. Brownlee, "Evaluation of the Railroad Valley playa for use in vicarious calibration," *Proc. SPIE Conf.*, Vol. 2818, 1996.
10. K. J. Thome, "Absolute radiometric calibration of Landsat-7 ETM+ using the reflectance-based method," *Remote Sensing of Environment*, **78**, pp. 27-38, 2001.
11. K. Thome, E. Whittington, N. Smith, P. Nandy, and E. Zalewski, "Ground-reference technique for the absolute calibration of MODIS," *Proceedings of SPIE*, Vol. 4135, pp. 51-59., 2000.
12. S. F. Biggar, D. I. Gellman, and P. N. Slater, "Improved evaluation of optical depth components from Langley plot data," *Rem. Sens. Env.*, Vol. 32, pp. 91-101, 1990.
13. K. J. Thome, B. M. Herman, and J. A. Reagan, "Determination of precipitable water from solar transmission," *J. Appl. Meteor.*, Vol. 31, pp. 157-165, 1992.